Beam Energy Dependence of Jet-Quenching Effects in Au + Au Collisions at $\sqrt{s_{NN}} = 7.7$, 11.5, 14.5, 19.6, 27, 39, and 62.4 GeV

L. Adamczyk,[1] J. R. Adams,[29] J. K. Adkins,[19] G. Agakishiev,[17] M. M. Aggarwal,[31] Z. Ahammed,[51] N. N. Ajitanand,[40] I. Alekseev,[15,26] D. M. Anderson,[42] R. Aoyama,[46] A. Aparin,[17] D. Arkhipkin,[3] E. C. Aschenauer,[3] M. U. Ashraf,[45] A. Attri,[31] G. S. Averichev,[17] X. Bai,[7] V. Bairathi,[27] K. Barish,[48] A. Behera,[40] R. Bellwied,[44] A. Bhasin,[16] A. K. Bhati,[31] P. Bhattarai,[43] J. Bielcik,[10] J. Bielcikova,[11] L. C. Bland,[3] I. G. Bordyuzhin,[15] J. Bouchet,[18] J. D. Brandenburg,[36] A. V. Brandin,[26] D. Brown,[23] I. Bunzarov,[17] J. Butterworth,[36] H. Caines,[55] M. Calderón de la Barca Sánchez,[5] J. M. Campbell,[29] D. Cebra,[5] I. Chakaberia,[3] P. Chaloupka,[10] Z. Chang,[42] N. Chankova-Bunzarova,[17] A. Chatterjee,[51] S. Chattopadhyay,[51] J. H. Chen,[39] X. Chen,[21] X. Chen,[37] J. Cheng,[45] M. Cherney,[9] W. Christie,[3] G. Contin,[22] H. J. Crawford,[4] S. Das,[7] L. C. De Silva,[9] R. R. Debbe,[3] T. G. Dedovich,[17] J. Deng,[38] A. A. Derevschikov,[33] L. Didenko,[3] C. Dilks,[32] X. Dong,[22] J. L. Drachenberg,[20] J. E. Draper,[5] L. E. Dunkelberger,[6] J. C. Dunlop,[3] L. G. Efimov,[17] N. Elsey,[53] J. Engelage,[4] G. Eppley,[36] R. Esha,[6] S. Esumi,[46] O. Evdokimov,[8] J. Ewigleben,[23] O. Eyser,[3] R. Fatemi,[19] S. Fazio,[3] P. Federic,[11] P. Federicova,[10] J. Fedorisin,[17] Z. Feng,[7] P. Filip,[17] E. Finch,[47] Y. Fisyak,[3] C. E. Flores,[5] J. Fujita,[9] L. Fulek,[1] C. A. Gagliardi,[42] D. Garand,[34] F. Geurts,[36] A. Gibson,[50] M. Girard,[52] D. Grosnick,[50] D. S. Gunarathne,[41] Y. Guo,[18] S. Gupta,[16] A. Gupta,[16] W. Guryn,[3] A. I. Hamad,[18] A. Hamed,[42] A. Harlenderova,[10] J. W. Harris,[55] L. He,[34] S. Heppelmann,[5] S. Heppelmann,[32] A. Hirsch,[34] G. W. Hoffmann,[43] S. Horvat,[55] X. Huang,[45] H. Z. Huang,[6] T. Huang,[28] B. Huang,[8] T. J. Humanic,[29] P. Huo,[40] G. Igo,[6] W. W. Jacobs,[14] A. Jentsch,[43] J. Jia,[3,40] K. Jiang,[37] S. Jowzaee,[53] E. G. Judd,[4] S. Kabana,[18] D. Kalinkin,[14] K. Kang,[45] D. Kapukchyan,[48] K. Kauder,[53] H. W. Ke,[3] D. Keane,[18] A. Kechechyan,[17] Z. Khan,[8] D. P. Kikoła,[52] C. Kim,[48] I. Kisel,[12] A. Kisiel,[52] L. Kochenda,[26] M. Kocmanek,[11] T. Kollegger,[12] L. K. Kosarzewski,[52] A. F. Kraishan,[41] L. Krauth,[48] P. Kravtsov,[26] K. Krueger,[2] N. Kulathunga,[44] L. Kumar,[31] J. Kvapil,[10] J. H. Kwasizur,[14] R. Lacey,[40] J. M. Landgraf,[3] K. D. Landry,[6] J. Lauret,[3] A. Lebedev,[3] R. Lednicky,[17] J. H. Lee,[3] C. Li,[37] W. Li,[39] Y. Li,[45] X. Li,[37] J. Lidrych,[10] T. Lin,[14] M. A. Lisa,[29] P. Liu,[40] F. Liu,[7] H. Liu,[14] Y. Liu,[42] T. Ljubicic,[3] W. J. Llope,[53] M. Lomnitz,[22] R. S. Longacre,[3] X. Luo,[7] S. Luo,[8] G. L. Ma,[39] L. Ma,[39] Y. G. Ma,[39] R. Ma,[3] N. Magdy,[40] R. Majka,[55] D. Mallick,[27] S. Margetis,[18] C. Markert,[43] H. S. Matis,[22] K. Meehan,[5] J. C. Mei,[38] Z. W. Miller,[8] N. G. Minaev,[33] S. Mioduszewski,[42] D. Mishra,[27] S. Mizuno,[22] B. Mohanty,[27] M. M. Mondal,[13] D. A. Morozov,[33] M. K. Mustafa,[22] Md. Nasim,[6] T. K. Nayak,[51] J. M. Nelson,[4] M. Nie,[39] G. Nigmatkulov,[26] T. Niida,[53] L. V. Nogach,[33] T. Nonaka,[46] S. B. Nurushev,[33] G. Odyniec,[22] A. Ogawa,[3] K. Oh,[35] V. A. Okorokov,[26] D. Olvitt, Jr.,[41] B. S. Page,[3] R. Pak,[3] Y. Pandit,[8] Y. Panebratsev,[17] B. Pawlik,[30] H. Pei,[7] C. Perkins,[4] P. Pile,[3] J. Pluta,[52] K. Poniatowska,[52] J. Porter,[22] M. Posik,[41] N. K. Pruthi,[31] M. Przybycien,[1] J. Putschke,[53] H. Qiu,[34] A. Quintero,[41] S. Ramachandran,[19] R. L. Ray,[43] R. Reed,[23] M. J. Rehbein,[9] H. G. Ritter,[22] J. B. Roberts,[36] O. V. Rogachevskiy,[17] J. L. Romero,[5] J. D. Roth,[9] L. Ruan,[3] J. Rusnak,[11] O. Rusnakova,[10] N. R. Sahoo,[42] P. K. Sahu,[13] S. Salur,[22] J. Sandweiss,[55] E. Sangaline,[5] M. Saur,[11] J. Schambach,[43] A. M. Schmah,[22] W. B. Schmidke,[3] N. Schmitz,[24] B. R. Schweid,[40] J. Seger,[9] M. Sergeeva,[6] R. Seto,[48] P. Seyboth,[24] N. Shah,[39] E. Shahaliev,[17] P. V. Shanmuganathan,[23] M. Shao,[37] M. K. Sharma,[16] A. Sharma,[16] W. Q. Shen,[39] Z. Shi,[22] S. S. Shi,[7] Q. Y. Shou,[39] E. P. Sichtermann,[22] R. Sikora,[1] M. Simko,[11] S. Singha,[18] M. J. Skoby,[14] D. Smirnov,[3] N. Smirnov,[55] W. Solyst,[14] L. Song,[44] P. Sorensen,[3] H. M. Spinka,[2] B. Srivastava,[34] T. D. S. Stanislaus,[50] M. Strikhanov,[26] B. Stringfellow,[34] T. Sugiura,[46] M. Sumbera,[11] B. Summa,[32] X. M. Sun,[7] Y. Sun,[37] X. Sun,[7] B. Surrow,[41] D. N. Svirida,[15] A. H. Tang,[3] Z. Tang,[37] A. Taranenko,[26] T. Tarnowsky,[25] A. Tawfik,[54] J. Thäder,[22] J. H. Thomas,[22] A. R. Timmins,[44] D. Tlusty,[36] T. Todoroki,[3] M. Tokarev,[17] S. Trentalange,[6] R. E. Tribble,[42] P. Tribedy,[3] S. K. Tripathy,[13] B. A. Trzeciak,[10] O. D. Tsai,[6] T. Ullrich,[3] D. G. Underwood,[2] I. Upsal,[29] G. Van Buren,[3] G. van Nieuwenhuizen,[3] A. N. Vasiliev,[33] F. Videbæk,[3] S. Vokal,[17] S. A. Voloshin,[53] A. Vossen,[14] F. Wang,[34] Y. Wang,[7] G. Wang,[6] Y. Wang,[45] J. C. Webb,[3] G. Webb,[3] L. Wen,[6] G. D. Westfall,[25] H. Wieman,[22] S. W. Wissink,[14] R. Witt,[49] Y. Wu,[18] Z. G. Xiao,[45] G. Xie,[37] W. Xie,[34] Z. Xu,[3] N. Xu,[22] Y. F. Xu,[39] Q. H. Xu,[38] J. Xu,[7] Q. Yang,[37] C. Yang,[38] S. Yang,[3] Y. Yang,[28] Z. Ye,[8] Z. Ye,[8] L. Yi,[55] K. Yip,[3] I.-K. Yoo,[35] N. Yu,[7] H. Zbroszczyk,[52] W. Zha,[37] X. P. Zhang,[45] S. Zhang,[39] J. B. Zhang,[7] J. Zhang,[22] Z. Zhang,[39] S. Zhang,[37] J. Zhang,[21] Y. Zhang,[37] J. Zhao,[34] C. Zhong,[39] L. Zhou,[37] C. Zhou,[39] Z. Zhu,[38] X. Zhu,[45] and M. Zyzak[12]

(STAR Collaboration)

[1]*AGH University of Science and Technology, FPACS, Cracow 30-059, Poland*
[2]*Argonne National Laboratory, Argonne, Illinois 60439, USA*

[3]Brookhaven National Laboratory, Upton, New York 11973, USA
[4]University of California, Berkeley, California 94720, USA
[5]University of California, Davis, California 95616, USA
[6]University of California, Los Angeles, California 90095, USA
[7]Central China Normal University, Wuhan, Hubei 430079, China
[8]University of Illinois at Chicago, Chicago, Illinois 60607, USA
[9]Creighton University, Omaha, Nebraska 68178, USA
[10]Czech Technical University in Prague, FNSPE, Prague, 115 19, Czech Republic
[11]Nuclear Physics Institute AS CR, Prague, 250 68, Czech Republic
[12]Frankfurt Institute for Advanced Studies FIAS, Frankfurt 60438, Germany
[13]Institute of Physics, Bhubaneswar 751005, India
[14]Indiana University, Bloomington, Indiana 47408, USA
[15]Alikhanov Institute for Theoretical and Experimental Physics, Moscow 117218, Russia
[16]University of Jammu, Jammu 180001, India
[17]Joint Institute for Nuclear Research, Dubna, 141 980, Russia
[18]Kent State University, Kent, Ohio 44242, USA
[19]University of Kentucky, Lexington, Kentucky 40506-0055, USA
[20]Lamar University, Physics Department, Beaumont, Texas 77710, USA
[21]Institute of Modern Physics, Chinese Academy of Sciences, Lanzhou, Gansu 730000, China
[22]Lawrence Berkeley National Laboratory, Berkeley, California 94720, USA
[23]Lehigh University, Bethlehem, Pennsylvania 18015, USA
[24]Max-Planck-Institut fur Physik, Munich 80805, Germany
[25]Michigan State University, East Lansing, Michigan 48824, USA
[26]National Research Nuclear University MEPhI, Moscow 115409, Russia
[27]National Institute of Science Education and Research, HBNI, Jatni 752050, India
[28]National Cheng Kung University, Tainan 70101, Taiwan
[29]Ohio State University, Columbus, Ohio 43210, USA
[30]Institute of Nuclear Physics PAN, Cracow 31-342, Poland
[31]Panjab University, Chandigarh 160014, India
[32]Pennsylvania State University, University Park, Pennsylvania 16802, USA
[33]Institute of High Energy Physics, Protvino 142281, Russia
[34]Purdue University, West Lafayette, Indiana 47907, USA
[35]Pusan National University, Pusan 46241, Korea
[36]Rice University, Houston, Texas 77251, USA
[37]University of Science and Technology of China, Hefei, Anhui 230026, China
[38]Shandong University, Jinan, Shandong 250100, China
[39]Shanghai Institute of Applied Physics, Chinese Academy of Sciences, Shanghai 201800, China
[40]State University of New York, Stony Brook, New York 11794, USA
[41]Temple University, Philadelphia, Pennsylvania 19122, USA
[42]Texas A&M University, College Station, Texas 77843, USA
[43]University of Texas, Austin, Texas 78712, USA
[44]University of Houston, Houston, Texas 77204, USA
[45]Tsinghua University, Beijing 100084, China
[46]University of Tsukuba, Tsukuba, Ibaraki 305-8571, Japan,
[47]Southern Connecticut State University, New Haven, Connecticut 06515, USA
[48]University of California, Riverside, California 92521, USA
[49]United States Naval Academy, Annapolis, Maryland 21402, USA
[50]Valparaiso University, Valparaiso, Indiana 46383, USA
[51]Variable Energy Cyclotron Centre, Kolkata 700064, India
[52]Warsaw University of Technology, Warsaw 00-661, Poland
[53]Wayne State University, Detroit, Michigan 48201, USA
[54]World Laboratory for Cosmology and Particle Physics (WLCAPP), Cairo 11571, Egypt
[55]Yale University, New Haven, Connecticut 06520, USA

(Received 11 July 2017; revised manuscript received 29 March 2018; published 19 July 2018)

We report measurements of the nuclear modification factor R_{CP} for charged hadrons as well as identified $\pi^{+(-)}$, $K^{+(-)}$, and $p(\bar{p})$ for Au + Au collision energies of $\sqrt{s_{\mathrm{NN}}} = 7.7$, 11.5, 14.5, 19.6, 27, 39, and 62.4 GeV. We observe a clear high-p_T net suppression in central collisions at 62.4 GeV for charged hadrons which evolves smoothly to a large net enhancement at lower energies. This trend is driven by the evolution

of the pion spectra but is also very similar for the kaon spectra. While the magnitude of the proton R_{CP} at high p_T does depend on the collision energy, neither the proton nor the antiproton R_{CP} at high p_T exhibit net suppression at any energy. A study of how the binary collision-scaled high-p_T yield evolves with centrality reveals a nonmonotonic shape that is consistent with the idea that jet quenching is increasing faster than the combined phenomena that lead to enhancement.

DOI: 10.1103/PhysRevLett.121.032301

Evidence has been presented that high-energy heavy-ion collisions form a dense, nearly perfect, strongly interacting, deconfined partonic liquid called quark-gluon plasma (QGP) [1–4]. This state of matter is thought to have dominated the Universe prior to the hadron epoch [5]. Quantifying the properties of the QGP is necessary for describing the QCD phase diagram [6], as well as constraining parameters in cosmological models that describe the evolution of the Universe along a trajectory through the QCD phase diagram [7]. Just as the Universe followed a particular trajectory through the QCD phase diagram, so do high-energy nuclear collisions. The particular path for each collision depends on the collision energy [8]. High-energy heavy-ion collisions reach approximate thermalization and form media with low initial baryon chemical potentials (μ_B) that are expected to remain low throughout their evolution. This means that the trajectory passes through the region where a smooth crossover is predicted by theory [9,10]. Lower collision energies have been shown to produce higher μ_B [11,12]. A first-order phase transition is predicted at sufficiently high μ_B [13,14] which would mean the existence of a critical end point [15]. A beam energy scan (BES) program at the Relativistic Heavy-Ion Collider (RHIC) was proposed to further explore the QCD phase diagram, including a search for the critical point, and to demonstrate that signatures for QGP formation turn off at sufficiently low collision energies [16]. The STAR Collaboration has recently published moments of net-proton and net-charge fluctuations in the BES as part of its critical point search [17,18] with no evidence for the critical point within current uncertainties. The future BES II program at the RHIC will increase the acceptance and reduce the uncertainties for these measurements. Implicit in the interpretation of these analyses was the requirement that a QGP be formed in the collisions at energies whose trajectories through the QCD phase diagram would pass near the critical point. Analyses are being carried out to determine at what collision energies signatures of QGP formation vanish. The beam-energy dependence of charge separation along the magnetic field in Au + Au collisions is already published with results consistent with models featuring chiral symmetry restoration down to $\sqrt{s_{NN}} = 11.5$ GeV [19]. In another study, the third harmonic of azimuthal correlations was measured as a function of the collision energy and the number of participating nucleons ($\langle N_{part}\rangle$) [20]. Models have shown that the third harmonic is sensitive to the low viscosity of the QGP phase [21–23], and this measurement showed that the third harmonic persisted down to $\sqrt{s_{NN}} = 7.7$ GeV for high-$\langle N_{part}\rangle$ collisions. Both of these low-p_T results are consistent with QGP being formed for $\sqrt{s_{NN}} \geq 11.5$ GeV so that the critical point would be directly accessible down to this collision energy. While each of these measurements is compelling on their own, it is by constructing a body of independent measurements that we will gain confidence that the QGP is being formed at these low collision energies. The measurements presented here focus on high-p_T probes of QGP formation: in particular, partonic energy loss, or jet quenching.

High-p_T partons, the forebears of jets, are produced early in the collision, and while moving through QGP volume they lose energy via strong interactions. This process is called jet quenching [24,25]. Jet quenching has contributions from collisional and radiative energy loss with strong force analogs to the processes described in chapters 13 and 14, respectively, of Jackson's iconic text [26]. This would be expected to lead to a depletion, or suppression, of high-p_T hadrons in the final state.

One method of observing this suppression is with the nuclear modification factor R_{CP}, which is defined by Eq. (1):

$$R_{CP} = \frac{\langle N_{coll}\rangle_{peripheral}}{\langle N_{coll}\rangle_{central}} \frac{\left(\frac{d^2N}{dp_T d\eta}\right)_{central}}{\left(\frac{d^2N}{dp_T d\eta}\right)_{peripheral}}. \quad (1)$$

Here, N_{coll} is the average number of binary collisions within a centrality bin and can be estimate using a Glauber Monte Carlo calculation [27]. If heavy-ion collisions were just a collection of N_{coll} independent $p + p$-like collisions, then R_{CP} would be unity for the entire p_T range. Effects that increase the number of particles per binary collision in central heavy-ion collisions relative to $p + p$ or peripheral collisions are called enhancement effects and lead to $R_{CP} > 1$, while those that decrease the number of particles are called suppression effects and lead to $R_{CP} < 1$. Therefore, R_{CP} quantifies whether enhancement or suppression effects are dominating but not the magnitude of each separately. Equation (1) compares the number of particles measured in small impact parameter (central) collisions, where the mean path length through any produced medium would be longer, with large impact

parameter (peripheral) collisions where the shorter in-medium path lengths should result in less energy loss. High-p_T suppression was observed at top RHIC energies, $\sqrt{s_{\rm NN}} = 130$ and 200 GeV, soon after the RHIC began running [1–4] and later at higher energy experiments at the Large Hadron Collider [28,29].

High-p_T suppression is expected to vanish at low collision energies, where the energy density becomes too low to produce a sufficiently large and long-lived QGP. Another effect that may lead toward suppression at the lower collision energies is the European Muon Collaboration (EMC) effect, a suppression of per nucleon cross sections in heavier nuclei relative to lighter nuclei for Bjorken $x > 0.3$, first measured with deep inelastic scattering by the EMC [30]. While they measured an impact parameter averaged nuclear modification of the parton distribution function, we are interested in the impact parameter dependence of this effect [31]. Experimentally quantifying this and other possible cold nuclear matter (CNM) effects requires $p + p$ and $p(d) + \mathrm{Au}$ reference data for the BES I energies.

Several physical effects could enhance hadron production in specific kinematic ranges, concealing the turn-off of the suppression due to jet quenching. One such effect is the Cronin effect, a CNM effect first observed in asymmetric collisions between heavy and light nuclei, where an enhancement of high-p_T particles was measured rather than suppression [32–34]. It has been demonstrated that the enhancement from the Cronin effect grows larger as the impact parameter is reduced [35,36]. Other processes in heavy-ion collisions such as radial flow and particle coalescence may also cause enhancement [37]. This is due to the effect of increasing particle momenta in steeply falling spectra. A larger shift of more abundant low-p_T particles to higher momenta in more central events—such as from radial flow, p_T broadening, or coalescence—would lead to an enhancement of the $R_{\rm CP}$. These enhancement effects would be expected to compete with jet quenching, which shifts high-p_T particles toward lower momenta. This means that measuring a nuclear modification factor to be greater than unity does not automatically lead us to conclude that a QGP is not formed. Disentangling these competing effects may be accomplished with complementary measurements, such as event plane-dependent nuclear modification factors [38], or through other methods like the one developed in this Letter.

In this Letter, we report measurements sensitive to partonic energy loss using data collected in the 2010, 2011, and 2014 RHIC runs by the STAR detector [39]. STAR is a large acceptance detector whose tracking and particle identification for this analysis were provided by its time projection chamber (TPC) [40] and time-of-flight (TOF) [41] detectors. These detectors lie within a 0.5 T magnetic field used to bend the paths of charged particles for momentum determination. Minimum bias-triggered events were selected by requiring coincident signals at forward and backward rapidities in the vertex position detectors (VPDs) [42] with a signal at midrapidity in the TOF. The VPDs also provide the start time for the TOF system, with the TOF's total timing resolution below 100 ps [41]. Events were selected if their position in the beam direction was within 30 cm of the TPC's center and if their transverse vertex position was within 1 cm of the mean transverse position for all events. The charged multiplicity, used for determining event centrality, was also corrected for variations in the detector response as a function of the vertex position in the beam direction [43,44]. Tracks were accepted if their distance of closest approach to the reconstructed vertex position was less than 1 cm, they had greater than 15 points measured in the TPC out of a maximum of 45, and the number of points used in track reconstruction divided by the number of possible points was greater than 0.52. The p_T- and species-dependent tracking efficiencies in the TPC were determined by embedding simulated tracks into real events for each energy and centrality [40]. The charged hadron tracking efficiency was taken as the weighted average of the fits to the single species efficiencies with the weights provided by fits to the corrected spectra of each species. Daughters from weak decay feeddown were removed from all spectra. The corrections for absorption and feeddown were determined by passing events generated in UrQMD [45] through a STAR detector simulation. Charged tracks in $|\eta| < 0.5$ and identified particles with $|y| < 0.25$ were accepted for this analysis. Particle identification was performed using both energy loss in the TPC (dE/dx) and time-of-flight information ($1/\beta$).

The overall scaling systematic uncertainty (33%–43%) for the $R_{\rm CP}$ measurements is dominated by the determination of $N_{\rm coll}$ and the total cross section, which is driven by trigger inefficiency and vertex reconstruction efficiency in peripheral events. Point-to-point systematic uncertainties arise from the determination of the single particle efficiency (5% for the p_T range studied here), momentum resolution (2%), and feeddown (p_T- and centrality-dependent with a range of 4%–7%). These systematic uncertainties are highly correlated as a function of the centrality and p_T with the different sources of uncertainty added in quadrature. Point-to-point systematic uncertainties for identified species have an additional contribution from uncertainties in particle identification that grow larger as the dE/dx and $1/\beta$ bands for the different species merge at higher momenta. The contribution from particle identification to the systematic uncertainties is small (1%–3%) at low p_T and large (up to 9%) at high p_T.

Figure 1 shows the $\sqrt{s_{\rm NN}}$ and p_T dependence of charged hadron $R_{\rm CP}$ constructed with data from (0–5)% and (60–80)% event centralities. The $R_{\rm CP}$ is found to be lowest at the highest beam energy studied and increases progressively from a suppression regime at 62.4 GeV to a

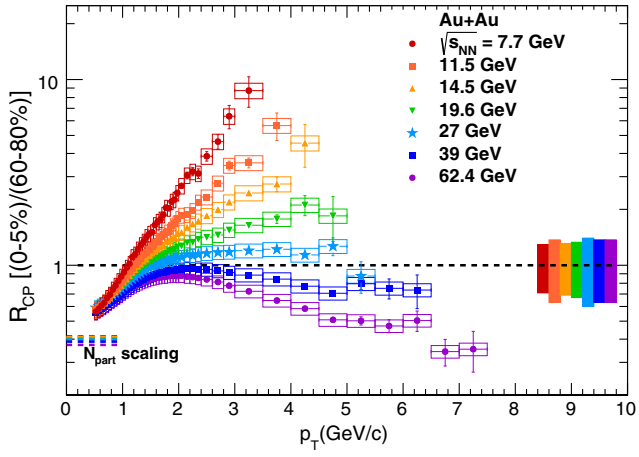

FIG. 1. Charged hadron R_{CP} for RHIC BES energies. The uncertainty bands at unity on the right side of the plot correspond to the p_T-independent uncertainty in N_{coll} scaling with the color in the band corresponding to the color of the data points for that energy. The vertical uncertainty bars correspond to statistical uncertainties and the boxes to systematic uncertainties.

pronounced enhancement at the lowest beam energies. This enhancement may have contributions from Cronin-type interactions [32–34], radial flow [37], and the relative dominance of coalescence versus fragmentation for hadronization [37]. The number of participant nucleons ($\langle N_{part} \rangle$) scaling, which is expected to be more appropriate for bulk particle production at lower p_T, is shown on the y axis. This plot demonstrates the turn-off of net suppression for high-p_T hadrons produced in central collisions relative to those produced in peripheral collisions. This meets, for this signature of QGP formation, one of the goals of the BES [16]. Figure 1 clearly demonstrates that enhancement effects become very large at lower energies. Therefore, in order to identify at what collision energy QGP is formed, more sensitive observables are required. The next step is to quantify more sensitive probes that could reveal potential evidence of jet quenching at lower collision energies.

In order to extract R_{CP} for identified hadrons, the particle rapidity density (dN/dy) is used in Eq. (1) instead of $dN/d\eta$. Figure 2 shows R_{CP} as a function of p_T for feeddown subtracted identified particles at different collision energies. While net enhancement of high-p_T particles is observed at all energies for p and $\bar{p}$, high-p_T $\pi^{+(-)}$ are suppressed for both 39 and 62.4 GeV, which drives the trends observed in charged hadrons. $K^{+(-)}$ have a similar energy dependence to $\pi^{+(-)}$ but show less net suppression. The R_{CP} of protons seems to turn over for the highest two energies. The large suppression of low-p_T $\bar{p}$ R_{CP} is consistent with a picture of annihilation prior to kinetic freeze-out [46]. Suppression in R_{CP} of pions persists to lower collision energies than that of charged hadrons; this is likely due to a smaller enhancement from the Cronin effect, radial flow, and coalescence for pions than protons.

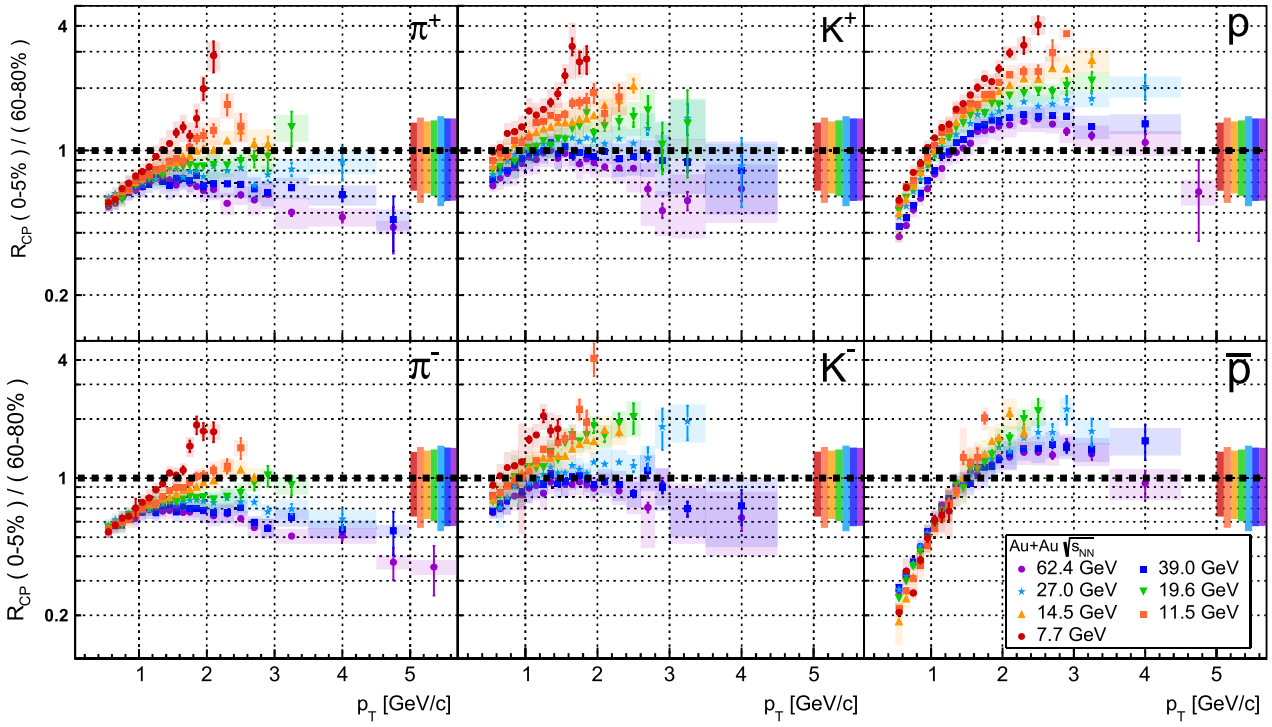

FIG. 2. Identified particle R_{CP} for RHIC BES energies. The colored shaded boxes describe the point-to-point systematic uncertainties. The uncertainty bands at unity on the right side of the plot correspond to the p_T-independent uncertainty in N_{coll} scaling with the color in the band corresponding to the color of the data points for that energy.

These measurements of $\pi^{+(-)}$ $R_{\rm CP}$ are consistent with measurements of π^0 $R_{\rm AA}$ in Au + Au collisions at $\sqrt{s_{\rm NN}} \geq 39$ GeV [47] and with π^0 $R_{\rm CP}$ in Pb + Pb collisions at $\sqrt{s_{\rm NN}} = 17.3$ GeV [48]. However, while earlier measurements demonstrated the disappearance of net suppression, the results presented here extend to lower collision energies where a strong net enhancement is observed.

A measurement of $R_{\rm CP}$ takes the ratio of $N_{\rm coll}$-scaled spectra from two different centralities [49]. A differential method for studying jet quenching is to look at how the $N_{\rm coll}$-scaled spectra trend with centrality for a high-p_T bin via

$$Y(\langle N_{\rm part}\rangle) = \frac{B}{\langle N_{\rm coll}\rangle}\frac{d^2N}{dp_T d\eta}(\langle N_{\rm part}\rangle), \qquad (2)$$

where B is a normalization term defined such that $Y(50) = 1$ for each energy and is used to simplify the comparison from one energy to the next. This is equivalent to taking the numerator from $R_{\rm CP}$ and plotting it versus the centrality so that the peripheral bin contents are in the first bin at low $\langle N_{\rm part}\rangle$ and the central bin's contents are in the last point at high $\langle N_{\rm part}\rangle$. Examining the full centrality evolution allows for the disentanglement of whether the processes leading to enhancement increase faster or slower than the processes leading toward suppression as a function of the centrality. While both jet quenching and enhancement effects increase in strength with increasing $\langle N_{\rm part}\rangle$, if there is a faster growth of quenching, it would manifest itself in decreasing $Y(\langle N_{\rm part}\rangle)$ trends.

Figure 3 shows the charged hadron yield per binary collision as a function of $\langle N_{\rm part}\rangle$ for $3 < p_T < 3.5$ GeV/c in the left panel and for $4 < p_T < 4.5$ GeV/c in the right panel. The left panel corresponds to the highest p_T bin of the $\sqrt{s_{\rm NN}} = 7.7$ GeV data and the right panel to the highest p_T bin of the $\sqrt{s_{\rm NN}} = 14.5$ GeV data. The 200 GeV points are from STAR data taken in 2010 and analyzed with the same procedure as the BES points. At $\sqrt{s_{\rm NN}} = 200$ GeV, $Y(\langle N_{\rm part}\rangle)$ decreases monotonically with increasing $N_{\rm part}$. This implies that the increase in jet quenching from peripheral to central collisions is stronger than the increase for effects which lead to enhancement. For a given $\langle N_{\rm part}\rangle$, $Y(\langle N_{\rm part}\rangle)$ always decreases with increasing $\sqrt{s_{\rm NN}}$. At $\sqrt{s_{\rm NN}} = 7.7$ GeV, $Y(\langle N_{\rm part}\rangle)$ increases monotonically with increasing $N_{\rm part}$. At 11.5 GeV, $Y(\langle N_{\rm part}\rangle)$ still increases monotonically with increasing $N_{\rm part}$ but less rapidly than at 7.7 GeV. As $\sqrt{s_{\rm NN}}$ increases, a peak develops in $Y(\langle N_{\rm part}\rangle)$ which persists until $\sqrt{s_{\rm NN}} = 62.4$ GeV. For $\sqrt{s_{\rm NN}} \geq 14.5$ GeV, a suppression in $Y(\langle N_{\rm part}\rangle)$ is observed for $\langle N_{\rm part}\rangle \approx 350$ relative to lower $\langle N_{\rm part}\rangle$ bins. Finally, at $\sqrt{s_{\rm NN}} = 200$ GeV, $Y(\langle N_{\rm part}\rangle)$ is suppressed for $\langle N_{\rm part}\rangle \geq 50$ and decreases monotonically with increasing $\langle N_{\rm part}\rangle$. The $\sqrt{s_{\rm NN}} = 14.5$ GeV data in the right panel in Fig. 3

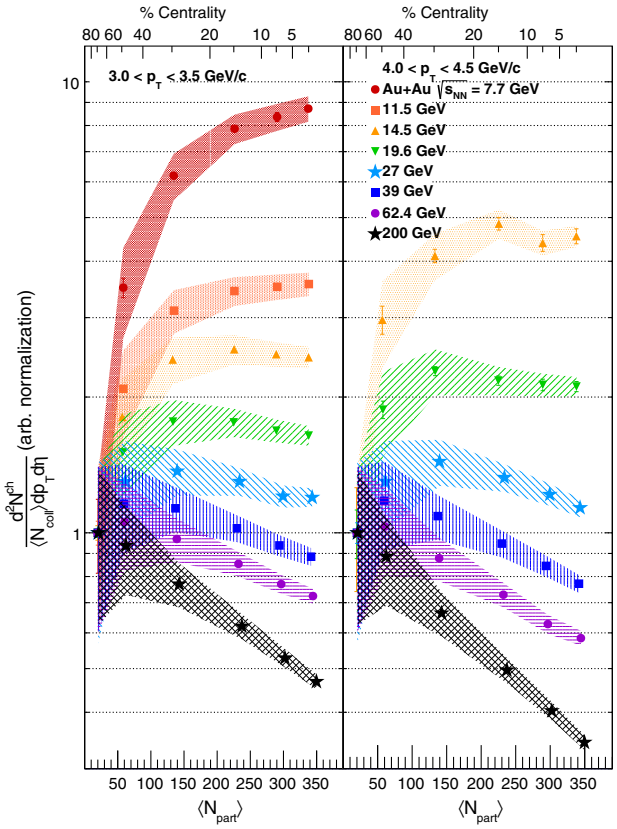

FIG. 3. Charged hadron $Y(\langle N_{\rm part}\rangle)$ for two ranges of p_T. Statistical uncertainty bars are included, mostly smaller than point size, as well as shaded bands to indicate systematic uncertainties.

shows a clear peak in $Y(\langle N_{\rm part}\rangle)$ at $\langle N_{\rm part}\rangle \approx 230$. This implies that enhancement effects increase faster than suppression effects for $\langle N_{\rm part}\rangle < 250$ at this energy. However, for $\langle N_{\rm part}\rangle > 250$, suppression effects increase at a similar rate or slightly faster than enhancement effects. In fact, if the systematic errors are taken to be 100% correlated, which is reasonable over this $N_{\rm part}$ range, then the yields at $\langle N_{\rm part}\rangle \approx 350$ are significantly suppressed relative to the yields at $\langle N_{\rm part}\rangle \approx 230$. This may be interpreted as medium-induced jet quenching decreasing high-p_T yields in central collisions at $\sqrt{s_{\rm NN}} \gtrsim 14.5$ GeV. As we move to higher energies, we find evidence for jet quenching in less central collisions. This does not exclude the possibility of QGP formation in the 7.7 and 11.5 GeV data sets but simply that enhancement effects increase faster than quenching effects for all centralities at these energies. This hadronic dominance at lower energies is consistent with measurements of other QGP signatures in the BES [19,20,50].

In summary, net high-p_T suppression persists for charged hadron $R_{\rm CP}$ for $\sqrt{s_{\rm NN}} > 39$ GeV. Mesons show a trend from $R_{\rm CP} < 1$ at the highest energies to $R_{\rm CP} > 1$ at the lowest energies, while baryons show an $R_{\rm CP} > 1$ at high

p_T for all energies in the RHIC BES. This indicates that pion R_{CP} is a cleaner observable for medium-induced jet quenching with pion R_{CP} suppressed for $\sqrt{s_{\mathrm{NN}}} > 27$ GeV. Partonic energy loss may still occur at lower $\sqrt{s_{\mathrm{NN}}}$ with Cronin-like enhancement effects competing with suppression effects. For this reason, the observable $Y(\langle N_{\mathrm{part}}\rangle)$ is considered in addition to R_{CP}. Finally, using $Y(\langle N_{\mathrm{part}}\rangle)$, we have measured suppression of charged hadrons in 0%–5% central events relative to more peripheral events for $\sqrt{s_{\mathrm{NN}}} \gtrsim 14.5$ GeV. This high-p_T result does not rule out the possibility that QGP is also formed in $\sqrt{s_{\mathrm{NN}}} < 14.5$ GeV, since $Y(\langle N_{\mathrm{part}}\rangle)$ is sensitive only to whether suppression effects increase faster than enhancement effects with increasing $\langle N_{\mathrm{part}}\rangle$. Instead, it frames a consistent picture with previous measurements to support a model where QGP is formed in central collisions at $\sqrt{s_{\mathrm{NN}}} > 14.5$ GeV.

We thank the RHIC Operations Group and RCF at BNL, the NERSC Center at LBNL, and the Open Science Grid consortium for providing resources and support. This work was supported in part by the Office of Nuclear Physics within the U.S. DOE Office of Science, the U.S. National Science Foundation, the Ministry of Education and Science of the Russian Federation, National Natural Science Foundation of China, Chinese Academy of Science, the Ministry of Science and Technology of China and the Chinese Ministry of Education, the National Research Foundation of Korea, GA and MSMT of the Czech Republic, Department of Atomic Energy and Department of Science and Technology of the Government of India, the National Science Centre of Poland, National Research Foundation, the Ministry of Science, Education and Sports of the Republic of Croatia, RosAtom of Russia, and German Bundesministerium fur Bildung, Wissenschaft, Forschung and Technologie (BMBF) and the Helmholtz Association.

[1] I. Arsene *et al.* (BRAHMS Collaboration), Nucl. Phys. **A757**, 1 (2005).
[2] B. Back *et al.* (PHOBOS Collaboration), Nucl. Phys. **A757**, 28 (2005).
[3] J. Adams *et al.* (STAR Collaboration), Nucl. Phys. **A757**, 102 (2005).
[4] K. Adcox *et al.* (PHENIX Collaboration), Nucl. Phys. **A757**, 184 (2005).
[5] M. J. Fromerth, I. Kuznetsova, L. Labun, J. Letessier, and J. Rafelski, Acta Phys. Pol. B **43**, 2261 (2012).
[6] M. Gyulassy and L. McLerran, Nucl. Phys. **A750**, 30 (2005).
[7] B. McInnes, Phys. Rev. D **93**, 043544 (2016).
[8] L. Adamczyk *et al.* (STAR Collaboration), Phys. Rev. C **96**, 044904 (2017).
[9] Y. Aoki, G. Endrodi, Z. Fodor, S. D. Katz, and K. K. Szabo, Nature (London) **443**, 675 (2006).
[10] S. Borsanyi, Z. Fodor, C. Hoelbling, S. D. Katz, S. Krieg, C. Ratti, and K. K. Szabo (Wuppertal-Budapest Collaboration), J. High Energy Phys. 09 (2010) 073.
[11] J. Cleymans, H. Oeschler, K. Redlich, and S. Wheaton, Phys. Rev. C **73**, 034905 (2006).
[12] A. Andronic, P. Braun-Munzinger, and J. Stachel, Phys. Lett. B **673**, 142 (2009); **678**, 516(E) (2009).
[13] S. Ejiri, Phys. Rev. D **78**, 074507 (2008).
[14] E. S. Bowman and J. I. Kapusta, Phys. Rev. C **79**, 015202 (2009).
[15] M. A. Stephanov, Prog. Theor. Phys. Suppl. **153**, 139 (2004); [Int. J. Mod. Phys. A **20**, 4387 (2005)].
[16] M. Aggarwal *et al.* (STAR Collaboration), arXiv: 1007.2613.
[17] L. Adamczyk *et al.* (STAR Collaboration), Phys. Rev. Lett. **112**, 032302 (2014).
[18] L. Adamczyk *et al.* (STAR Collaboration), Phys. Rev. Lett. **113**, 092301 (2014).
[19] L. Adamczyk *et al.* (STAR Collaboration), Phys. Rev. Lett. **113**, 052302 (2014).
[20] L. Adamczyk *et al.* (STAR Collaboration), Phys. Rev. Lett. **116**, 112302 (2016).
[21] B. Muller, Acta Phys. Pol. B **38**, 3705 (2007).
[22] W. A. Zajc, Nucl. Phys. **A805**, 283c (2008).
[23] C. Gale, S. Jeon, B. Schenke, P. Tribedy, and R. Venugopalan, Phys. Rev. Lett. **110**, 012302 (2013).
[24] J. Bjorken, Fermi National Accelerator Laboratory Report No. FERMILAB-PUB-82-059-THY, 1982.
[25] X.-N. Wang and M. Gyulassy, Phys. Rev. Lett. **68**, 1480 (1992).
[26] J. D. Jackson, *Classical Electrodynamics* (Wiley, New York, 1975).
[27] M. L. Miller, K. Reygers, S. J. Sanders, and P. Steinberg, Annu. Rev. Nucl. Part. Sci. **57**, 205 (2007).
[28] S. Chatrchyan *et al.* (CMS Collaboration), Eur. Phys. J. C **72**, 1945 (2012).
[29] B. B. Abelev *et al.* (ALICE Collaboration), Eur. Phys. J. C **74**, 3108 (2014).
[30] J. J. Aubert *et al.* (European Muon Collaboration), Phys. Lett. B **123**, 275 (1983).
[31] I. Helenius, K. Eskola, H. Honkanen, and C. Salgado, Nucl. Phys. **A904–905**, 999c (2013).
[32] J. Cronin, H. J. Frisch, M. J. Shochet, J. P. Boymond, P. A. Piroué, and R. L. Sumner, Phys. Rev. D **11**, 3105 (1975).
[33] D. Antreasyan, J. W. Cronin, H. J. Frisch, M. J. Shochet, L. Kluberg, P. A. Piroue, and R. L. Sumner, Phys. Rev. D **19**, 764 (1979).
[34] P. B. Straub *et al.*, Phys. Rev. Lett. **68**, 452 (1992).
[35] I. Vitev, Phys. Lett. B **562**, 36 (2003).
[36] A. Accardi and M. Gyulassy, Phys. Lett. B **586**, 244 (2004).
[37] V. Greco, C. M. Ko, and P. Levai, Phys. Rev. C **68**, 034904 (2003).
[38] A. Adare *et al.* (PHENIX Collaboration), Phys. Rev. C **87**, 034911 (2013).
[39] K. Ackermann *et al.* (STAR Collaboration), Nucl. Instrum. Methods Phys. Res., Sect. A **499**, 624 (2003).
[40] M. Anderson *et al.*, Nucl. Instrum. Methods Phys. Res., Sect. A **499**, 659 (2003).
[41] W. Llope (STAR Collaboration), Nucl. Instrum. Methods Phys. Res., Sect. A **661**, S110 (2012).

[42] W. J. Llope *et al.*, Nucl. Instrum. Methods Phys. Res., Sect. A **759**, 23 (2014).
[43] S. Horvat, Ph.D. thesis, Yale University, 2017.
[44] E. Sangaline, Ph.D. thesis, University of California–Davis, 2014.
[45] S. Bass *et al.*, Prog. Part. Nucl. Phys. **41**, 255 (1998).
[46] B. Shiva Kumar, S. V. Greene, and J. T. Mitchell, Phys. Rev. C **50**, 2152 (1994).
[47] A. Adare *et al.* (PHENIX Collaboration), Phys. Rev. Lett. **109**, 152301 (2012).
[48] M. M. Aggarwal *et al.* (WA98 Collaboration), Eur. Phys. J. C **23**, 225 (2002).
[49] See Supplemental Material at http://link.aps.org/supplemental/10.1103/PhysRevLett.121.032301 for the p_T spectra and centrality determination, which includes Refs. [50,51].
[50] L. Adamczyk *et al.* (STAR Collaboration), Phys. Rev. Lett. **110**, 142301 (2013).
[51] B. B. Back *et al.* (PHOBOS Collaboration), Phys. Rev. C **70**, 021902(R) (2004).